Modified Nonlinear Integral Sliding Mode Control for Satellite Attitude Stabilization Using Magnetically Suspended Gimbaled Momentum Wheel*

Jingbo Wei and Kun Liu
College of Aerospace Science and Engineering
National University of Defense Technology
Changsha, People's Republic of China, 410073
weijingbo615@foxmail.com and liukun@nudt.edu.cn

Gianmarco Radice
Aerospace Technology Center
University of Glasgow
Scotland G12 8QQ, United Kingdom
Gianmarco.Radice@glasgow.ac.uk

Abstract **- This paper treats the attitude stabilization problem for satellite using only one MSGMW (Magnetically Suspended Gimbaled Momentum Wheel). To start, the coupled dynamic model of satellite and MSGMW is defined and simplified based on the fact that the attitude errors are small during the mission mode that the MSGMW services. In order to improve the dynamic performance, reduce the steady state error and avoid the chattering phenomenon, a modified integral chattering-free sliding mode controller with a nonlinear integral function and a saturation function is introduced. Lyapunov theory is employed to prove the convergence characteristic outside the boundary layer and the terminal convergence characteristic inside the boundary layer. A numerical simulation example is employed to show the effectiveness and suitability of the proposed controller.**

Index Terms - Attitude Stabilization, MSGMW, MNISMC, Integral Sliding Mode Control

I. Introduction

Three-axis stabilized satellites are widely used for Earth observation, communication and navigation missions. A common attitude control architecture consists of a momentum wheel for pitch stabilization and thrusters for roll and yaw stabilization. The MSGMW, with its angular momentum aligned along the pitch axis, can also provide control torques along the other two axes, like a Double Gimbal Control Moment Gyro but the gimbal angles are limited in a small range. Once the satellite establishes an initial attitude after the damping phase, the errors are usually very small, and a MSGMW can be used to stabilize all the three axes thus reducing fuel consumption, increase the service life of the satellite and enhance the attitude precision for roll and yaw axis.

The use of MSGMW for spacecraft attitude control has been the subject of different studies [1]~[6]. A robust controller is proposed for attitude stabilization using a 2-DOF method and applied to a Sun observation mission [2]. MSGMW is used to cope with the perturbations induced by scanning actuators in Ref. [3]. The non-linearities and on-orbit stability problems for MSGMW are studied in Ref. [4] and [5] respectively. A stabilization controller is designed in Ref. [6] under the condition that the pitch attitude information is missing.

All the above studies design a controller and prove the stability based on classic control theory, however, the external disturbances and the uncertainties of the main angular momentum are not considered. SMC (Sliding Mode Controller) has shown to be a promising approach displaying strong robustness in the case of parameter uncertainties and perturbations. In order to avoid chattering and terminal convergence issues-the main drawbacks of a traditional SMC, saturation functions, integral sliding mode control, and terminal sliding mode control have been proposed. Reference [7] generally summarizes the development and the characteristics of SMC, as well as its possible modifications. The attitude stabilization and maneuvering problems are studied using various SMCs in Ref. [8]~[15] showing the proper robustness for space applications, where in particular Ref.[13] and [14] use terminal sliding mode theory to solve the final convergence problem and Ref. [15] combines sliding mode theory and adaptive theory to study the saturation problem during the attitude control process. The ISMC (Integral Sliding Mode Control) is firstly proposed by Chern [6] and can compensate the uncertainties in the system, remove the steady state error and enhance the robustness [17~19]. Some ISMC application problems are studied in Ref. [20~23] which show the promising results.

This paper will tackle the satellite attitude stabilization problem using only one MSGMW as actuator and a Modified Nonlinear Integral Sliding Mode Controller (MNISMC) is designed based on the theory in Ref. [24].

The rest of the paper is structured as follows. Sections II defines the coupled nonlinear dynamic model and introduces some simplifications based on small angular displacements. The control strategy is presented in Section III, while the MNISMC is defined in Section IV. A numerical example is given in Section V and Section VI concludes the whole paper.

II Modeling And Simplification

A satellite is orbiting the Earth on a circular orbit and it is in an Earth-pointing three axis-stabilization mode as shown in Figure 1. The orbit frame is selected to be attitude reference frame which is defined as: z axis is in the nadir direction, y axis is in the negative orbit normal direction and x axis

* This work is partially supported by the National Nature Science Foundation of China (Grant No. 61304036, 11301173).

completes the right hand orthogonal system. The attitude angles of the satellite, yaw ψ, pitch θ, roll φ, are defined as the three Euler angles when the orbit frame rotates to the body frame by a 3-2-1 rotation sequence. The MSGMW is mounted as follows: the rotating direction of the rotor aligns with –y axis of the orbit frame and the wheel gimbals by small angles (no more than 2 degrees) in x and z axis and the gimballing angles are defined as γ in x axis and δ in z axis. The angular velocity of the body frame, namely the satellite angular velocity, with respect to the inertial frame, is defined as $\vec{\boldsymbol{\omega}}_B$, and the relative angular velocity of MSGMW with respect to the satellite body frame is defined as $\vec{\boldsymbol{\omega}}_r$. Then the absolute angular velocity of MSGMW is: $\vec{\boldsymbol{\omega}}_W = \vec{\boldsymbol{\omega}}_B + \vec{\boldsymbol{\omega}}_r$. The attitude kinematics equations of satellite and MSGMW are given in satellite body frame by:

$$\begin{cases} \boldsymbol{\omega}_B = R_1(\varphi)\{\dot{\boldsymbol{\varphi}} + R_2(\theta)[\dot{\boldsymbol{\theta}} + R_3(\psi)(\dot{\boldsymbol{\psi}} + \boldsymbol{\omega}_0]\} \\ \boldsymbol{\omega}_r = R_1(\gamma)\{\dot{\boldsymbol{\gamma}} + R_3(\delta)[\dot{\boldsymbol{\delta}} + R_2(\Omega t + \Omega_0)\Omega]\} \end{cases} \tag{1}$$

According to the moment of momentum theorem, the coupled dynamic equation of satellite and MSGMW is given by

$$\frac{\partial \vec{\boldsymbol{H}}_B}{\partial t} + \vec{\boldsymbol{\omega}}_B \times \vec{\boldsymbol{H}}_B + \boldsymbol{T}_S + \frac{\partial \vec{\boldsymbol{H}}_W}{\partial t} + \vec{\boldsymbol{\omega}}_B \times \vec{\boldsymbol{H}}_W + \vec{\boldsymbol{\omega}}_r \times \vec{\boldsymbol{H}}_W + \boldsymbol{T}_W = \boldsymbol{T}_d\,, \tag{2}$$

where, $\vec{\boldsymbol{H}}_B$ is the angular momentum of satellite, $\vec{\boldsymbol{H}}_W$ the angular momentum of MSGMW, $\boldsymbol{T}_d$ is the vector of external disturbance torques, $\boldsymbol{T}_S$, $\boldsymbol{T}_W$ are the internal torques from MSGMW towards satellite and from satellite towards MSGMW respectively such that: $\boldsymbol{T}_W = -\boldsymbol{T}_S$.

In the satellite body frame, the momentums can be expressed in vector form as:

$$\begin{cases} \boldsymbol{H}_B = \boldsymbol{I}_S \boldsymbol{\omega}_B \\ \boldsymbol{H}_W = \boldsymbol{B}_{WS} \boldsymbol{J}_W \boldsymbol{B}_{WS}^{\mathrm{T}} \boldsymbol{\omega}_W = \boldsymbol{B}_{WS} \boldsymbol{J}_W \boldsymbol{B}_{WS}^{\mathrm{T}} (\boldsymbol{\omega}_B + \boldsymbol{\omega}_r) \end{cases}, \tag{3}$$

where, $\boldsymbol{B}_{WS}$ is the rotation matrix from rotor frame to satellite body frame. Substituting (3) into (2) yields

$$\begin{aligned} &\boldsymbol{I}_S \dot{\boldsymbol{\omega}}_B + [\boldsymbol{\omega}_B \times] \boldsymbol{I}_S \boldsymbol{\omega}_B + \boldsymbol{T}_S - \boldsymbol{T}_d \\ &= -\left[\frac{\partial}{\partial t}(\boldsymbol{B}_{WS} \boldsymbol{J}_W \boldsymbol{B}_{WS}^{\mathrm{T}})\right](\boldsymbol{\omega}_B + \boldsymbol{\omega}_r) - (\boldsymbol{B}_{WS} \boldsymbol{J}_W \boldsymbol{B}_{WS}^{\mathrm{T}})(\dot{\boldsymbol{\omega}}_B + \dot{\boldsymbol{\omega}}_r)\,, \\ &-\left[(\boldsymbol{\omega}_B + \boldsymbol{\omega}_r)\times\right] \boldsymbol{B}_{WS} \boldsymbol{J}_W \boldsymbol{B}_{WS}^{\mathrm{T}} (\boldsymbol{\omega}_B + \boldsymbol{\omega}_r) - \boldsymbol{T}_W \end{aligned} \tag{4}$$

where, $[\boldsymbol{\omega}_B \times]$ is the adjoint matrix of vector $\boldsymbol{\omega}_B$ defined as follows:

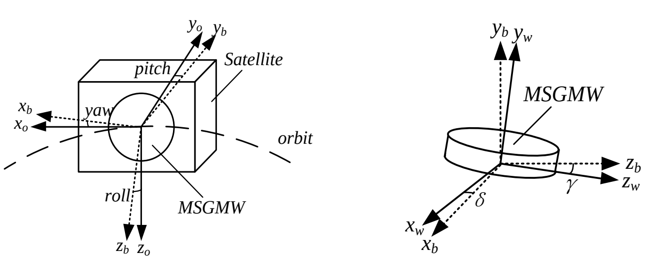

Fig. 1 Satellite Attitude and Movement of MSGMW

$$[\boldsymbol{\omega}_B \times] = \begin{bmatrix} 0 & -\omega_{Bz} & \omega_{By} \\ \omega_{Bz} & 0 & -\omega_{Bx} \\ -\omega_{By} & \omega_{Bx} & 0 \end{bmatrix}$$

Since we are assuming that the attitude angles are all small, the kinematics equations can be simplified as:

$$\begin{aligned} \boldsymbol{\omega}_B &= \begin{bmatrix} \dot{\varphi} - \omega_0 \psi & \dot{\theta} - \omega_0 & \dot{\psi} + \omega_0 \varphi \end{bmatrix}^{\mathrm{T}} \\ \boldsymbol{\omega}_r &= \begin{bmatrix} \dot{\gamma} - \Omega\delta & -\Omega & \dot{\delta} + \Omega\gamma \end{bmatrix}^{\mathrm{T}} \end{aligned} \tag{5}$$

Furthermore, assuming that both satellite and MSGMW are symmetric, then

$$\begin{aligned} \boldsymbol{I}_S &= diag\left(\begin{bmatrix} I_x & I_y & I_z \end{bmatrix}\right) \\ \boldsymbol{J}_W &= diag\left(\begin{bmatrix} J_x & J_y & J_z \end{bmatrix}\right) \end{aligned}, \tag{6}$$

Substituting (5) and (6) into the kinematics and dynamics equations and simplifying the results yields the final simplified dynamics model. It is important to remark that the simplification process is reasonable and widely used in previous studies and engineering practice [1~6].

$$\begin{cases} I_x \ddot{\varphi} + H_y \dot{\psi} + \omega_0 H_y \varphi = -J_x \ddot{\delta} - H_y \dot{\gamma} - \omega_0 H_y \delta + T_{dx} \\ I_y \ddot{\theta} = \dot{H}_y + T_{dy} \\ I_z \ddot{\psi} - H_y \dot{\varphi} + \omega_0 H_y \psi = -J_z \ddot{\gamma} + H_y \dot{\delta} - \omega_0 H_y \gamma + T_{dz} \end{cases} \tag{7}$$

where, $H_y = J_y \dot{\Omega}$ is the main angular momentum of MSGMW.

III. Control Strategy Analysis

From (7) it can be seen that the pitch axis is decoupled from the other two axes and hence it can be analyzed independently. We will there focus our analysis and discussion on the yaw and roll axis. Since the gimbal angles of MSGMW are also coupled as shown in (7), we need to introduce two virtual control variables T_{cx}, T_{cz}, as:

$$\begin{cases} T_{cx} = -J_x \ddot{\delta} - H_y \dot{\gamma} - \omega_0 H_y \delta \\ T_{cz} = -J_z \ddot{\gamma} + H_y \dot{\delta} - \omega_0 H_y \gamma \end{cases}. \tag{8}$$

So, the dynamics model becomes:

$$\begin{cases} I_x \ddot{\varphi} + H_y \dot{\psi} + \omega_0 H_y \varphi = T_{cx} + T_{dx} \\ I_z \ddot{\psi} - H_y \dot{\varphi} + \omega_0 H_y \psi = T_{cz} + T_{dz} \end{cases}. \tag{9}$$

The effectiveness of the virtual control variables T_{cx}, T_{cz} relies on tracking the desired gimbal angles integrated from T_{cx}, T_{cz} according to (8).

In order to simplify the calculation procedure of desired gimbal angles of MSGMW, and considering the fact that $J_x \ll H_y$, the second-order terms in (8) can be ignored. So the desired gimbal angles will be calculated by:

$$\begin{cases} T_{cx} \doteq -H_y \dot{\gamma} - \omega_0 H_y \delta \\ T_{cz} \doteq H_y \dot{\delta} - \omega_0 H_y \gamma \end{cases}. \tag{10}$$

It is very important to notice that the control bandwidth of MSGMW is generally above 10 KHz, which is considerably larger than that of the satellite attitude control

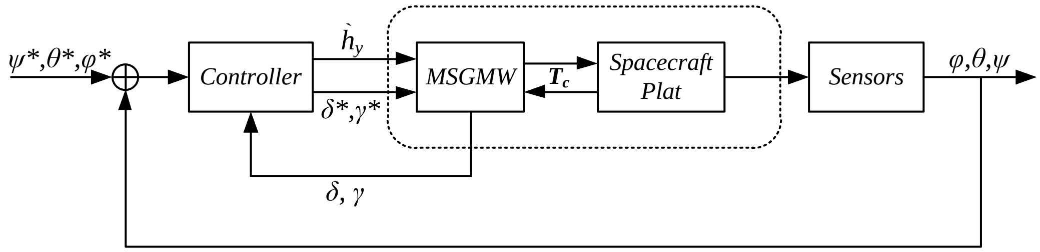

Fig. 2 Control Process Block Diagram

loop – usually no more than 20 Hz. So we can take the gimbal tracking process as a gain that the MSGMW can track the desired angles immediately and accurately. As a result, the attitude control law can be designed independently.

IV CONTROL LAW DESIGN

Since the pitch is a SISO second-order integral loop and hence it is very easy to design the controller, so the main task of this paper is to design a robust controller for the other two axes.

Select the state vectors as $\boldsymbol{x}_1 = [\varphi \quad \psi]^{\mathrm{T}}$, $\boldsymbol{x}_2 = [\dot{\varphi} \quad \dot{\psi}]^{\mathrm{T}}$, then the system state equation becomes:

$$\begin{cases} \dot{\boldsymbol{x}}_1 = \boldsymbol{x}_2 \\ \dot{\boldsymbol{x}}_2 = \boldsymbol{M}^{-1}(\boldsymbol{K}\boldsymbol{x}_1 + \boldsymbol{C}\boldsymbol{x}_2 + \boldsymbol{t}_c + \boldsymbol{d}) \end{cases}, \tag{11}$$

where,

$$\boldsymbol{C} = \begin{bmatrix} 0 & H_y \\ -H_y & 0 \end{bmatrix} \ \boldsymbol{K} = \omega_0 \begin{bmatrix} H_y & 0 \\ 0 & H_y \end{bmatrix} \ \boldsymbol{M} = \begin{bmatrix} I_x & 0 \\ 0 & I_z \end{bmatrix}$$

$$\boldsymbol{t_c} = [T_{cx} \quad T_{cz}]^{\mathrm{T}} \quad \boldsymbol{d} = [T_{dx} \quad T_{dz}]^{\mathrm{T}}$$

where the real attitude angle and angular rate are measured by inertial sensors and gyros respectively. The first and second terms in the second equation of (11) represent the system dynamics while the third term is the control. The external disturbances are represented by the fourth term.

The attitude error is given by:

$$\boldsymbol{e} = \boldsymbol{x}_1 - \boldsymbol{x}_{1r} = \begin{bmatrix} e_\varphi & e_\psi \end{bmatrix}^{\mathrm{T}}. \tag{12}$$

Before finalizing the controller design, the following assumptions are given:

Assumption 1: There is a feedback error ΔH between the real momentum H_y and the measured one $\hat{H}_y$, but the error is bounded as

$$\left| H_y - \hat{H}_y \right| \le \delta_H , \tag{13}$$

so, the induced error of matrix $\boldsymbol{C}$ and $\boldsymbol{K}$ is bounded as follows

$$\begin{cases} \tilde{\boldsymbol{C}} = \boldsymbol{C} - \hat{\boldsymbol{C}} \\ \tilde{\boldsymbol{K}} = \boldsymbol{K} - \hat{\boldsymbol{K}} \end{cases}. \tag{14}$$

then, the maximum eigenvalues of $\tilde{\boldsymbol{C}}$ and $\tilde{\boldsymbol{K}}$ are given by

$$\begin{cases} \lambda_{\max,\tilde{\boldsymbol{C}}} = \delta_H \\ \lambda_{\max,\tilde{\boldsymbol{K}}} = \omega_0 \delta_H \end{cases}. \tag{15}$$

Assumption 2: The disturbance is also bounded as

$$\|\boldsymbol{d}\| \le \delta_d . \tag{16}$$

A Modified Nonlinear Integral Sliding Mode Function

In order to enhance the performance of a traditional sliding mode controller, a modified nonlinear integral sliding mode function is introduced

$$\begin{cases} \boldsymbol{s} = \dot{\boldsymbol{e}} + k_p \boldsymbol{e} + k_I \boldsymbol{\sigma}(\boldsymbol{e}) \\ \dot{\boldsymbol{\sigma}}(\boldsymbol{e}) = \boldsymbol{g}(\boldsymbol{e}) \end{cases}, \tag{17}$$

where, $\boldsymbol{s} = [s_\varphi \quad s_\psi]^{\mathrm{T}}$, k_p, k_I are both positive constant and $\boldsymbol{g}(\boldsymbol{e}) = [g(e_\varphi) \quad g(e_\psi)]^{\mathrm{T}}$, the nonlinear function $g(\lambda)$ is defined as

$$g(\lambda) = \begin{cases} \beta & \lambda \ge \beta \\ \beta \sin(\pi\lambda/2\beta) & |\lambda| < \beta \\ -\beta & \lambda \le -\beta \end{cases}. \tag{18}$$

From (18), $g(\lambda)$ has following characteristics: $g(\lambda) = 0$ if and only if $\lambda = 0$; when $|\lambda| < \beta$, then $g(\lambda)$ is a strictly monotone increasing function; when $|\lambda| \ge \beta$, $g(\lambda)$ is saturated by β which is positive a constant.

A curve of $g(\lambda)$ when $\lambda = 1$ is given by Fig. 3. It is apparent that when $|\lambda| \ge \beta$ the integral item in (17) will be slowed down by the saturation characteristic which would result in an improvement of the dynamic performance of the closed-loop system.

B Control Law Design and Analysis

The control law is given by Theorem 1 and the convergence of the proposed sliding function is proved by Theorem 2 as follows.

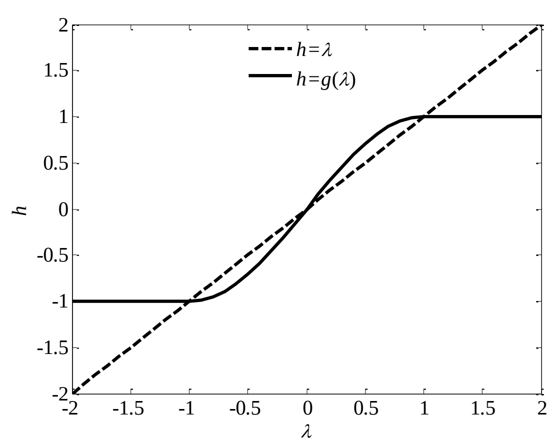

Fig. 3 Integral saturation function $g(\lambda)$

Theorem 1: For the system described by (11), if a sliding mode function is selected by (17) and the control law is designed with an exponential approaching law:

$$\boldsymbol{t}_c = \hat{\boldsymbol{t}}_c - \boldsymbol{c}(\boldsymbol{x}_1, \boldsymbol{x}_2, t)\mathrm{sat}(\boldsymbol{s}, \mu) - k_s \boldsymbol{s} + \boldsymbol{M}\ddot{\boldsymbol{x}}_{1r}, \tag{19}$$

where, μ is the bounded value of the saturation function, and the equivalent control law $\hat{\boldsymbol{t}}_c$ is given by

$$\hat{\boldsymbol{t}}_c = -\hat{\boldsymbol{K}}\boldsymbol{x}_1 - \hat{\boldsymbol{C}}\boldsymbol{x}_2 - \boldsymbol{M}[k_p \dot{\boldsymbol{e}} + k_I \boldsymbol{g}(\boldsymbol{e})], \tag{20}$$

and the switching gain matrix is

$$\boldsymbol{c}(\boldsymbol{x}_1, \boldsymbol{x}_2, t) = diag(\lambda_{\max,\tilde{\boldsymbol{K}}}|\boldsymbol{x}_1| + \lambda_{\max,\tilde{\boldsymbol{C}}}|\boldsymbol{x}_2| + \boldsymbol{d}_{\sup} + \boldsymbol{\eta}), \tag{21}$$

the system will then converge exponentially to sliding mode.

Proof: The control law can be written as (22) when the system is outside the bounds.

$$\boldsymbol{t}_c = \hat{\boldsymbol{t}}_c - \boldsymbol{c}(\boldsymbol{x}_1, \boldsymbol{x}_2, t)\mathrm{sgn}(\boldsymbol{s}), \tag{22}$$

A Lyapunov function is selected as:

$$V_1 = \boldsymbol{s}^{\mathrm{T}}\boldsymbol{s}/2, \tag{23}$$

the time derivative of V_1 is

$$\begin{aligned}
\dot{V}_1 &= \boldsymbol{s}^{\mathrm{T}}\dot{\boldsymbol{s}} \\
&= \boldsymbol{s}^{\mathrm{T}}(\boldsymbol{M}_2^{-1}(\boldsymbol{K}\boldsymbol{x}_1 + \boldsymbol{C}\boldsymbol{x}_2 + \boldsymbol{t}_c + \boldsymbol{d}) - \ddot{\boldsymbol{y}} + k_p \boldsymbol{e}_2 + k_I \boldsymbol{g}(\boldsymbol{e}_1)) \\
&= \boldsymbol{s}^{\mathrm{T}}\boldsymbol{M}_2^{-1}(\tilde{\boldsymbol{K}}\boldsymbol{x}_1 + \tilde{\boldsymbol{C}}\boldsymbol{x}_2 + \boldsymbol{d} - \boldsymbol{c}(\boldsymbol{x}_1, \boldsymbol{x}_2, t)\mathrm{sgn}(\boldsymbol{s}) - k_s \boldsymbol{s}) \\
&\le abs(\boldsymbol{s}^{\mathrm{T}})\boldsymbol{M}_2^{-1}(|\tilde{\boldsymbol{K}}\boldsymbol{x}_1 + \tilde{\boldsymbol{C}}\boldsymbol{x}_2 + \boldsymbol{d}| - (\lambda_{\max,\tilde{\boldsymbol{K}}}|\boldsymbol{x}_1| + \lambda_{\max,\tilde{\boldsymbol{C}}}|\boldsymbol{x}_2| + \boldsymbol{d}_{\sup}) - \boldsymbol{\eta}) \\
&\quad - k_s \boldsymbol{s}^{\mathrm{T}}\boldsymbol{M}_2^{-1}\boldsymbol{s} \\
&\le -abs(\boldsymbol{s}^{\mathrm{T}})\boldsymbol{M}_2^{-1}\boldsymbol{\eta} - k_s \boldsymbol{s}^{\mathrm{T}}\boldsymbol{M}_2^{-1}\boldsymbol{s}
\end{aligned} \tag{24}$$

It is very important to notice that the relation $|\tilde{\boldsymbol{K}}\boldsymbol{x}_1| \le \lambda_{\max,\tilde{\boldsymbol{K}}}|\boldsymbol{x}_1|$ is used above. So from (24), the system will reach the bounds exponentially. □

Define the sum of uncertain items in (11) as

$$\begin{cases} \boldsymbol{\zeta}(\boldsymbol{x}_1, \boldsymbol{x}_2, t) = \tilde{\boldsymbol{C}}\boldsymbol{x}_2 + \tilde{\boldsymbol{K}}\boldsymbol{x}_1 + \boldsymbol{d}(t) \\ \gamma_i = c_i(\boldsymbol{x}_1, \boldsymbol{x}_2, t)/\mu \quad i = 1, 2 \end{cases}. \tag{25}$$

Theorem 2 will prove that the system will converge to zero once inside the bounds.

Theorem 2: For the system (11), the control law is given by Theorem 1, the attitude error will converge to zero $\lim_{t\to\infty}\boldsymbol{e}(t) = 0$ if the uncertain sum $\boldsymbol{\zeta}(\boldsymbol{x}_1, \boldsymbol{x}_2, t)$ is a constant or ultimate constant disturbance, namely $\lim_{t\to\infty}\zeta_i(t) = l_i$, l_i is a constant, $i = 1, 2$.

Proof: The control law will be rewritten as (26) once the system reaches the bounds.

$$\boldsymbol{t}_c = \hat{\boldsymbol{t}}_c - \boldsymbol{c}(\boldsymbol{x}_1, \boldsymbol{x}_2, t)\boldsymbol{s}/\mu - k_s \boldsymbol{s} + \boldsymbol{M}_2\ddot{\boldsymbol{y}}, \tag{26}$$

Substituting (26) to (11) yields,

$$\dot{\boldsymbol{s}}(t) = \ddot{\boldsymbol{e}} + k_P \boldsymbol{e} + k_I g(\boldsymbol{e}) = \boldsymbol{\zeta}(\boldsymbol{x}_1, \boldsymbol{x}_2, t) - \gamma \boldsymbol{s}(t) = 0, \tag{27}$$

or

$$\dot{s}_i(t) = \ddot{e}_i + k_P e_i + k_I g(e_i) = \zeta_i(\boldsymbol{x}_1, \boldsymbol{x}_2, t) - \gamma s_i(t) = 0. \tag{28}$$

So,

$$s_i(p) = \frac{1}{p + \gamma_i}\zeta_i(p)。 \tag{29}$$

where, p is Laplace operator and from Final-Value Theorem

$$\begin{aligned}
\lim_{t\to\infty} s_i(t) &= \lim_{p\to 0}\frac{p}{p+\gamma_i}\zeta_i(p) = \lim_{p\to 0}\frac{1}{p+\gamma_i}\cdot\lim_{p\to 0} p\zeta_i(p) \\
&= \lim_{p\to 0}\frac{1}{p+\gamma_i}\cdot\lim_{t\to 0}\zeta_i(t) = \frac{l_i}{\gamma_i}
\end{aligned}, \tag{30}$$

So, when $t \to \infty$, $\dot{s}_i(t) \to 0$, namely

$$\lim_{t\to\infty}\ddot{\boldsymbol{e}} + k_p \dot{\boldsymbol{e}} + k_I \boldsymbol{g}(\boldsymbol{e}) = 0, \tag{31}$$

Another candidate Lyapunov function is

$$V_2 = \frac{1}{2}\dot{\boldsymbol{e}}^{\mathrm{T}}\dot{\boldsymbol{e}} + k_I(G(e_\varphi) + G(e_\psi)), \tag{32}$$

where the new function $G(\lambda)$ is defined as

$$G(\lambda) = \int_0^\lambda g(\eta)d\eta = \begin{cases} \dfrac{2\beta^2}{\pi}\left(1 - \cos\dfrac{\pi\lambda}{2\beta}\right) & \lambda \ge \beta \\ \beta\lambda - \dfrac{\pi-2}{\pi}\beta^2 & |\lambda| < \beta \\ -\beta\lambda - \dfrac{\pi-2}{\pi}\beta^2 & \lambda \le -\beta \end{cases}, \tag{33}$$

$G(\lambda) > 0$ if $\lambda \ne 0$ and $G(\lambda) = 0$ if and only if $\lambda = 0$. The derivative of $G(\lambda)$ with respect to λ is as same as(18). So V_2 is a Lyapunov function and its time derivative is given by

$$\begin{aligned}
\dot{V}_2 &= \dot{\boldsymbol{e}}^{\mathrm{T}}\ddot{\boldsymbol{e}} + k_I(g(e_\varphi)\dot{e}_\varphi + g(e_\psi)\dot{e}_\psi) \\
&= \dot{\boldsymbol{e}}^{\mathrm{T}}(-k_p\dot{\boldsymbol{e}} - k_I\boldsymbol{g}(\boldsymbol{e})) + k_I\dot{\boldsymbol{e}}^{\mathrm{T}}\boldsymbol{g}(\boldsymbol{e}) \\
&= -\dot{\boldsymbol{e}}^{\mathrm{T}}k_p\dot{\boldsymbol{e}} \le 0
\end{aligned}, \tag{34}$$

which means that when $t \to \infty$, then $\dot{s}_i(t) \to 0$, so $\lim_{t\to\infty}\dot{V}_2 = 0$, namely $\lim_{t\to\infty}\dot{\boldsymbol{e}}(t) = 0$. Then $\lim_{t\to\infty}\boldsymbol{e}(t) = 0$ according to (31). □

V. Numerical Simulation

In order to demonstrate the effectiveness and feasibility of the control law for the system, a numerical simulation is performed. The orbit angular velocity is $\omega_0 = 0.0011$ and the inertial parameters of satellite are $I_x = I_z = 300\mathrm{kg}\cdot\mathrm{m}^2$. The inertial parameters of MSGMW is given by $J_x = J_z = 0.02\mathrm{kg}\cdot\mathrm{m}^2$, $J_y = 0.04\mathrm{kg}\cdot\mathrm{m}^2$, the rotating speed is given by $\Omega = 12000 \pm 2000\mathrm{rpm}$, the maximum gimbal angle of MSGMW are 2.5° along both axes, and the nominal momentum of the MSGMW is $H_{y0} = J_y\Omega \doteq 25\mathrm{Nms}$ which is used in the feedback control law in the roll and yaw axes. The real angular momentum is defined as \` $H_y = 25 + 4\sin(\omega_0 t)$ Nms.

The control parameters in (19) are $k_P = 10$, $k_I = 2$, $\delta_H = 4$, $\delta_d = 0.001$, $k_s = 40$, $\beta = 0.00005$, $\eta = 0.5$, $\mu = 0.0006$.

The initial attitude state and the disturbance torques are given by

$$\begin{cases} \boldsymbol{x}_1(t_0) = \begin{bmatrix} 0.5^\circ & -0.4^\circ \end{bmatrix}^{\mathrm{T}} \\ \boldsymbol{x}_2(t_0) = \begin{bmatrix} 0 & 0 \end{bmatrix}^{\mathrm{T}} \ {}^\circ/\mathrm{s} \end{cases}, \boldsymbol{T}_d(t) = \begin{bmatrix} 8 + 2\sin(\omega_0 t) \\ 7 + 3\sin(\omega_0 t) \end{bmatrix} \times 10^{-4}\,\mathrm{Nm}$$

In order to show the performance of the proposed MNISMC is better than the traditional ISMC, two numerical examples using MNISMC and traditional ISMC respectively are conducted simultaneously, where the system and control parameters are all same in two examples with the only difference that $\boldsymbol{e}$ is used directly in the ISMC method instead of the nonlinear function $\boldsymbol{g}(\boldsymbol{e})$ in the integral term of the MNISMC controller.

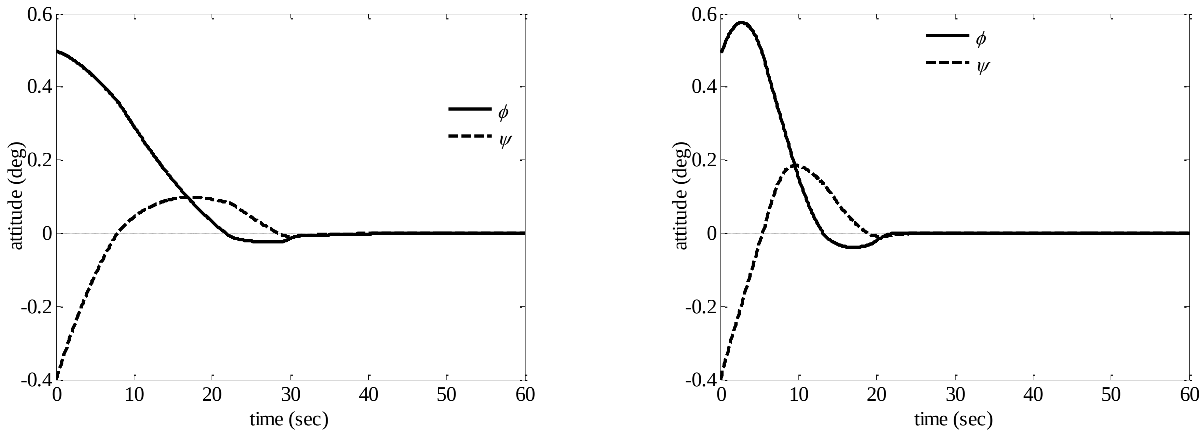

(a) MNISMC (b) ISMC

Fig. 4 Satellite attitude angles

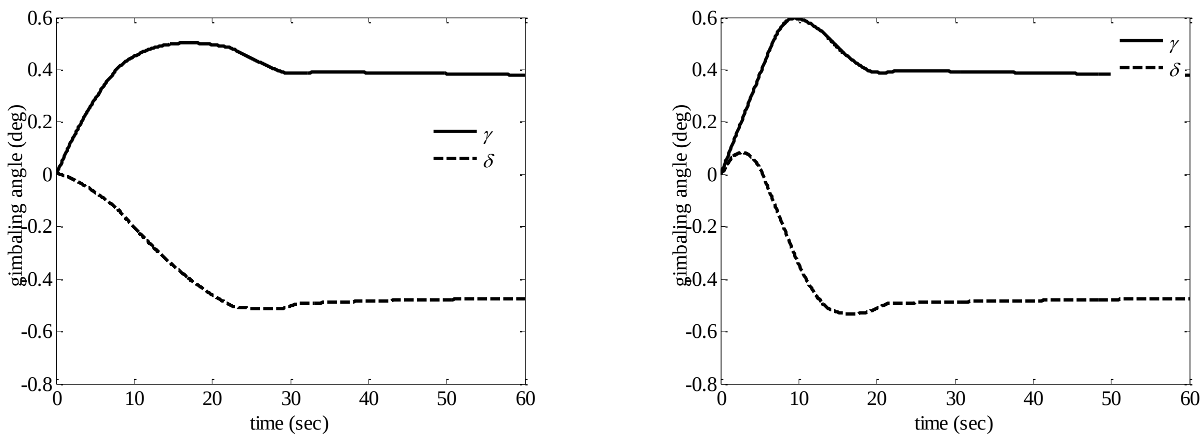

(a) MNISMC (b) ISMC

Fig. 5 MSGMW gimbal angles

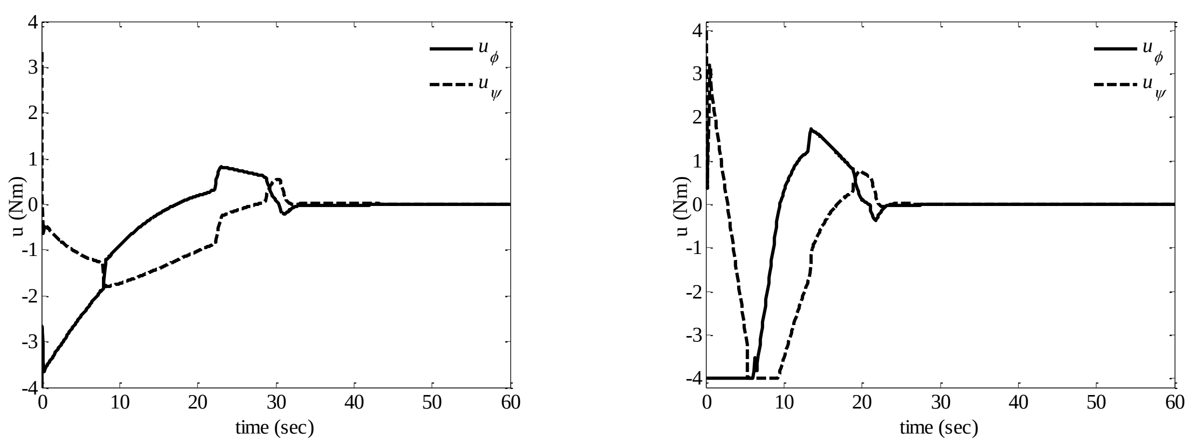

(a) MNISMC (b) ISMC

Fig. 6 Control torques

The simulation results are shown as Fig. 4 ~ Fig. 6. All the *(a)* parts in the figures are the results of the example using MNISMC and *(b)* parts are the ones using ISMC.

By using MNISMC, from Fig. 4(a), the attitude angles are converged in 40s without large overshooting phenomenon which is no more than 0.1° in yaw channel. As for ISMC, the attitude angles are converged in 30s which is quicker than MNISMC, but the overshooting phenomenon is considerable in roll channel at the initial moment and reaches 0.2° in yaw channel. From the above analysis, the MNISMC has improved the performance of the attitude control system with the cost of increasing the convergence time. It is very important to note that the final state converges to zero and there is no chattering phenomenon by taking advantages of the modification of the controller and the bound layer of the sliding function.

Fig. 5 gives the change process of deflection angles of MSGMW under both cases. In the MNISMC case, the deflection angles are no more than 0.5° . As for ISMC case, the maximum deflection angle increases to 0.6° . So the fast convergence process of ISMC is obtained by aggravating the movement of MSGMW which can also be seen in Fig. 6 which illustrates the control torques. From Fig. 6, the saturation arises in the ISMC case, but there is no saturation phenomenon in the MNISMC case.

By this token, under the same system and control parameters, the MNISMC method can reduce the overshooting, improve the control torque output and avoid the saturation with the price of long convergence time.

VI CONCLUSIONS

The attitude stabilization problem for satellite using only one MSGMW is studied in this paper. The coupled dynamic model of satellite and MSGMW is established firstly and simplified according to engineering practices. A modified nonlinear integral sliding mode control has been employed for the satellite attitude stabilization problem involving the momentum uncertainty and external disturbance by using only one MSGMW. This control method can improve the dynamic performance, reduce the steady state error and avoid the chattering phenomenon. The convergence characteristics are demonstrated by Lyapunov theory. A numerical simulation example is employed to show the effectiveness and superiority the proposed controller with respect to the traditional integrated sliding mode controller.

REFERENCES

[1]. Hashimoto T, Hamasaki T, Nakatani I, et al. "Attitude control system design of a satellite with a magnetically suspended momentum wheel based on two-degree-of-freedom control system theory". *AIAA Guidance, Navigation, and Control Conference*, pp. 9-11, 1993.

[2]. Bichler U J. "A double gimballed magnetic bearing momentum wheel for high pointing accuracy and vibration sensitive space applications". *Spacecraft Guidance, Navigation and Control Systems*, pp. 393-398, 1991.

[3]. Sawada H, Hashimoto T, Ninomiya K. "High-stability attitude control of satellites by magnetic bearing wheels". *Transactions Japan Society For Aeronautical and Space Sciences*, vol, 44, pp. 133-141, 2001.

[4]. Nam M R, Hashimoto T, Ninomiya K. "Control system design to cope with non-linearities of a magnetically suspended momentum wheel for satellites"//International Conference on Nonlinear Problems in Aviation and Aerospace, 1st, pp. 513-517, Daytona Beach, FL. 1996.

[5]. LIU Hu, FANG Jian-cheng, LIU Gang. "Research on the Stability of Magnetic Bearing System in Magnetically Suspended Momentum Wheel under on Orbit Condition". *Journal of Astronautics*, vol. 30, no. 2, pp. 625-630, 2009. (In Chinese).

[6]. LIU Hu, FANG Jian-cheng, LIU Gang. "Satellite Roll-yaw Axis Attitude Stable Control Based on Magnetically Suspended Momentum Wheel with Vernier Gimballing Capacity". *Journal of Astronautics*, vol. 31, no. 4, pp. 1063-1069, 2010. (In Chinese)

[7]. Liu J K, Sun F C. "Research and development on theory and algorithms of sliding mode control". *Kongzhi Lilun yu Yingyong/ Control Theory & Applications*, vol. 23, no. 3, pp. 407-418, 2007.

[8]. Lo S C, Chen Y P. "Smooth sliding-mode control for spacecraft attitude tracking maneuvers". *Journal of Guidance, Control, and Dynamics*, vol. 18, no. 6, pp. 1345-1349, 1995.

[9]. Crassidis J L, Markley F L. "Sliding mode control using modified Rodrigues parameters". *Journal of Guidance, Control, and Dynamics*, vol. 19, no. 6, pp. 1381-1383, 1996.

[10]. Terui F. "Position and attitude control of a spacecraft by sliding mode control"//American Control Conference, 1998. Proceedings of the 1998. IEEE, pp. 217-221, Jan. 1998.

[11]. Elmali H, Olgac N. "Robust output tracking control of nonlinear MIMO systems via sliding mode technique". *Automatica*, vol. 28, no. 1, pp. 145-151, 1992.

[12]. Hu Q, Ma G. "Variable structure control and active vibration suppression of flexible spacecraft during attitude maneuver". *Aerospace Science and Technology*, vol. 9, no. 4, pp. 307-317, 2005.

[13]. Wu S, Radice G, Gao Y, et al. "Quaternion-based finite time control for spacecraft attitude tracking". Acta Astronautica, vol. 69, no. 1, pp. 48-58, 2011.

[14]. Zou A M, Kumar K D, Hou Z G, et al. "Finite-time attitude tracking control for spacecraft using terminal sliding mode and Chebyshev neural network". *Systems, Man, and Cybernetics, Part B: Cybernetics, IEEE Transactions on*, vol. 41, no. 4, pp. 950-963, 2011.

[15]. Zhu Z, Xia Y, Fu M. "Adaptive sliding mode control for attitude stabilization with actuator saturation". *Industrial Electronics, IEEE Transactions on*, vol. 58, no. 10, pp. 4898-4907, 2011.

[16] Chern T L, Wu Y C. "Design of integral variable structure controller and application to electrohydraulic velocity servosystems"//IEE Proceedings D (Control Theory and Applications). IET Digital Library, vol. 138, no. 5, pp. 439-444, 1991.

[17]. Fridman L, Poznyak A, Bejarano F J. "Integral Sliding Mode Control"//Robust Output LQ Optimal Control via Integral Sliding Modes. Springer New York, pp. 11-20, 2014.

[18]. Laghrouche S, Plestan F, Glumineau A. Higher order sliding mode control based on integral sliding mode[J]. *Automatica*, vol. 43, no. 3, pp. 531-537, 2007.

[19]. Castaños F, Fridman L. "Analysis and design of integral sliding manifolds for systems with unmatched perturbations". *Automatic Control, IEEE Transactions on*, vol. 51, no. 5, pp. 853-858, 2006.

[20]. Baik I C, Kim K H, Youn M J. "Robust nonlinear speed control of PM synchronous motor using boundary layer integral sliding mode control technique". *Control Systems Technology, IEEE Transactions on*, vol. 8, no. 1, pp. 47-54, 2000.

[21]. Lee J H, Allaire P E, Tao G, et al. "Integral sliding-mode control of a magnetically suspended balance beam: analysis, simulation, and experiment". *Mechatronics, IEEE/ASME Transactions on*, vol. 6, no. 3, pp. 338-346, 2001.

[22]. Sam Y M, Osman J H S, Ghani M. "A class of proportional-integral sliding mode control with application to active suspension system". *Systems & control letters*, vol. 51, no. 3, pp. 217-223, 2004.

[23]. Shima T, Idan M, Golan O M. "Sliding-mode control for integrated missile autopilot guidance". *Journal of guidance, control, and dynamics*, vol. 29, no. 2, pp. 250-260, 2006.

[24] Li P, Zheng Z Q. "Sliding mode control approach with nonlinear integrator". *Control Theory & Applications*, vol. 28, no. 3, pp. 421-426, 2011. (In Chinese).